Biology of Reproduction, 2024, **110(2)**, 365–376
https://doi.org/10.1093/biolre/ioad158
Advance access publication date 16 November 2023
Research Article

In vivo dynamic volumetric imaging of mouse testis and epididymis with optical coherence tomography†

Kohei Umezu, Guzel R. Musina and Irina V. Larina*

Department of Integrative Physiology, Baylor College of Medicine, Houston, TX, USA

***Correspondence:** Department of Integrative Physiology, Baylor College of Medicine, One Baylor Plaza, Houston, TX 77030, USA. E-mail: larina@bcm.edu

†**Grant Support:** Supported by Japan Society for the Promotion of Science and National Institutes of Health grants R01EB027099 and R01HD096335.

Abstract

The implementation of live imaging in reproductive research is crucial for studying the physiological dynamics. Sperm transport is a highly dynamic process regulated by tubular contractions and luminal flows within the male reproductive tract. However, due to the lack of imaging techniques to capture these dynamics in vivo, there is little information on the physiological and biomechanical regulation of sperm transport through the male reproductive tract. Here, we present a functional in vivo imaging approach using optical coherence tomography, enabling live, label-free, depth-resolved, three-dimensional, high-resolution visualization of the mouse testis and epididymis. With this approach, we spatiotemporally captured tubular contractility in mouse testis and epididymis, as well as microstructures of these reproductive organs. Our findings demonstrated that the contraction frequency varies significantly depending on the epididymal regions, suggesting the spatial regulation of epididymal contractility. Furthermore, we implemented quantitative measurements of the contraction wave and luminal transport through the epididymal duct, revealing the physiological dynamics within the male reproductive tract. The results show that the contraction wave propagates along the epididymal duct and the wave propagation velocity was estimated in vivo. In conclusion, this is the first study to develop in vivo dynamic volumetric imaging of the male reproductive tract, which allows for quantitative analysis of the dynamics associated with sperm transport. This study sets a platform for various studies investigating normal and abnormal male reproductive physiology as well as the pharmacological and environmental effects on reproductive functions in mouse models, ultimately contributing to a comprehensive understanding of male reproductive disorders.

Summary Sentence

In vivo three-dimensional live imaging using optical coherence tomography revealed the physiological dynamics within the male mouse reproductive tract associated with sperm transport.

Received: June 21, 2023. **Revised:** September 19, 2023. **Accepted:** November 9, 2023

Graphical Abstract

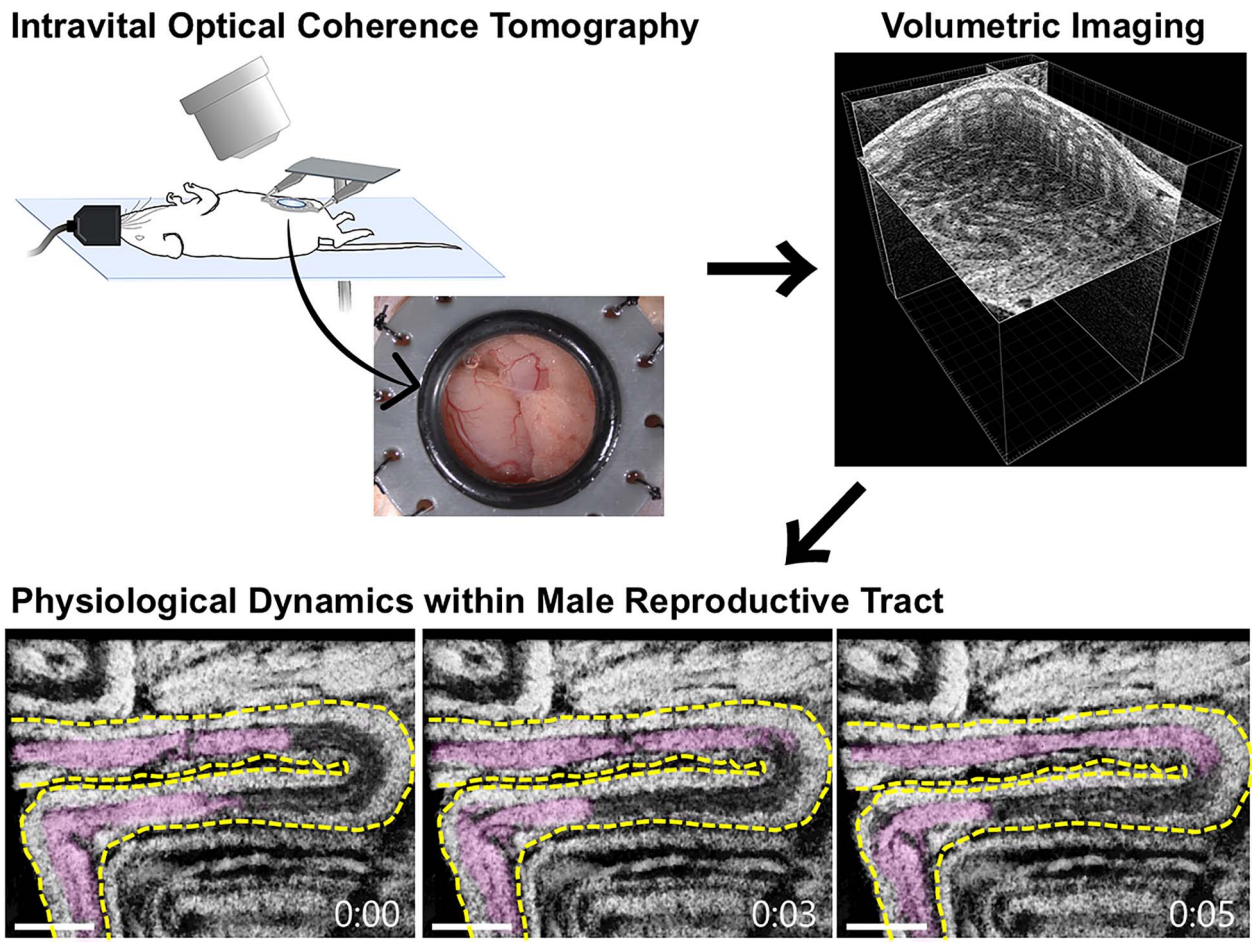

Key words: epididymis, in vivo imaging, intravital microscopy, optical coherence tomography, sperm transport, testis

Introduction

Spermatogenesis takes place inside the long, convoluted tubes called seminiferous tubules, which are packed within the testis [1]. Once sperm are produced and released from the testis, they are transported into the epididymis, which is the site of sperm maturation and storage. The epididymis is a duct-like organ that connects efferent ducts of the testes to vas deferens and is divided into three regions: the caput, corpus, and cauda. During their transfer through the epididymis, sperm undergo various physiological and biochemical modifications by interacting with the epithelium and luminal environment of the epididymal duct, enabling them to acquire potential motility and fertilizing ability [2].

Although sperm progressively acquire motility in the epididymis, they remain in a quiescent state in the male reproductive tract and become active after ejaculation through interactions with the surrounding environment within the female reproductive tract. Therefore, sperm are passively transported through the male reproductive tract, and thus the dynamics of the male reproductive tract are critical for the transport. In the testes, contractions of the seminiferous tubules and luminal fluid flow propel the immotile sperm in the seminiferous tubules through the rete testis into the epididymis [3]. Peritubular myoid cells are localized on the surface of the seminiferous tubules, and their contractility regulates the transport of sperm and luminal fluid within the seminiferous tubules [4]. Interestingly, the efferent ducts of the testes harbor ciliated cells, which are also involved in sperm transport through the tubules [5, 6]. In the epididymis, smooth muscle contractions are responsible for sperm transport [7]. The epididymal duct largely consists of the epithelial layer and the surrounding smooth muscle cell layer. The thickness of the smooth muscle cell layer increases along the epididymal duct from caput to cauda, but the frequency of contractions decreases from caput to cauda [8, 9]. Multiple molecules, such as noradrenaline, oxytocin, and vasopressin, are involved in regulating the contractility of smooth muscle cells in the epididymis [7, 10, 11]. Despite the accumulated knowledge on the molecular or hormonal regulation of this process, there is limited information on the dynamic aspect and regulation of sperm transport in the native state of the male reproductive tract, primarily due to the requirement for live imaging, which is still challenging. In this effort, Fleck et al. developed an in vivo imaging approach for the mouse testis using multiphoton microscopy, which enabled the visualization and quantification of seminiferous tubule contractions, inducing luminal transport inside the tubules [12]. Using this method, the authors demonstrated that ATP triggers the seminiferous tubule contractions that induce luminal transport inside

the tubules. Kanazawa et al. established an in vivo imaging method by employing a fluorescent-reporter mouse and two-photon excitation microscopy and investigated the luminal flow and sperm transfer in the seminiferous tubules [13]. Roy et al. reported an intravital imaging approach for the epididymis using transgenic mice with a fluorescent marker of basal cells in the epididymal epithelia and two-photon fluorescence microscopy [14]. This approach enabled the real-time visualization of axial motility of the basal cells in the mouse epididymis. These imaging-based studies clearly demonstrated the power of in vivo investigations in studying reproductive physiology. However, these studies also suggested the limitations of the developed methods. The bright-field microscopy is restricted to the top-view 2D visualization, while the confocal and multi-photon microscopies require fluorescent labels and the imaging is relatively slow because of their point-scanning nature. Also, the visualizations are limited to very superficial tissue layers due to the limited imaging depth. An in vivo imaging approach capable of dynamic, volumetric, quantitative assessment without the requirement for contrast agents is highly desirable for investigating the reproductive physiology associated with the tubular and luminal dynamics within the male reproductive tract. Such technology is currently not available, which served as a stimulus for the initiation of this study.

Optical coherence tomography (OCT) is a non-invasive, label-free, and depth-resolved imaging modality that provides a micro-scale spatial resolution (1–10 μm) with an imaging depth of approximately 2–3 mm in biological tissues [15]. Similar to ultrasound technology, its principle is based on measuring an echo delay in backscattered signals to define the spatial positions of the scatters within the sample, but it utilizes light rather than sound as used in the ultrasound. Optical coherence tomography can produce volumetric data over the field of view covering a few millimeters at a relatively high rate, enabling dynamic volumetric imaging. It relies on natural tissue contrast and does not require exogenous contrast agents. Due to these unique features, OCT is gaining popularity in various biological fields, including developmental biology [16] and reproductive biology [17, 18]. However, OCT applications toward the male reproductive system are extremely limited. Trottmann et al. employed 2D OCT for ex vivo imaging of the microstructure of the male reproductive organs in a bovine model [19]. Ramasamy et al. utilized an OCT-based 2D approach to detect sperm within seminiferous tubules in extracted rat testes [20]. Recently, we explored volumetric OCT for structural analysis of the extracted mouse male reproductive organs [21], demonstrating great potential for OCT in studying structural defects at cellular resolution. In contrast to males, in vivo applications of OCT are more advanced in the female reproductive system. Combined with an intravital imaging approach, OCT has provided valuable insights into the reproductive events, which were not accessible with other methods. Wang et al. reported an in vivo OCT imaging approach for dynamic volumetric investigations of individual sperm trajectories in the mouse oviduct, uncovering a wide variety of never-before-seen sperm behaviors in the native state [22]. For the imaging, the female mouse was anesthetized, and the reproductive tract was gently pulled out through a dorsal incision and stabilized with a clamp throughout the imaging to minimize movement artifacts caused by breathing. Using a similar approach, Wang et al. tracked the oocytes and preimplantation embryos in the native environment of the mouse oviduct, revealing spatially dependent dynamics of oocyte and embryo transport through the female reproductive tract [23]. Furthermore, OCT can be used to analyze cilia dynamics in the female reproductive system. By spatiotemporally mapping the cilia locations and cilia beat frequency along the mouse oviduct through the tissue layers in vivo, it has been demonstrated that cilia activity within the oviduct is temporally regulated and may play a crucial role in sperm and oocyte/embryo dynamics [24]. Establishing a similar intravital OCT imaging approach for male reproductive system is an intuitive next step to enable in vivo prolonged and potentially longitudinal investigations of male reproductive physiology.

The goal of this study was to develop an in vivo volumetric imaging method based on intravital OCT, which allows for dynamic and quantitative investigations of the physiological dynamics within the male reproductive system in mice. To achieve this, we implemented implantable imaging windows with a clear aperture, which allows one to bypass the skin and muscle layers for imaging while preserving a sealed semi-physiological environment. With this approach, we acquired volumetric visualizations of sperm transport and tubular dynamics within the mouse testis and epididymis in vivo, as well as quantified contractile waves along the epididymal duct.

Materials and methods

Animal procedures for in vivo imaging

All animal procedures have been approved by the Institutional Animal Care and Use Committee at Baylor College of Medicine, and all experiments in this study were conducted following the approved guidelines and protocols.

Young (7–14 weeks old) and aged (13–19 months old) wild-type CD1 male mice were used in this study. For in vivo imaging, a one-time surgery was performed to implant the imaging window (Figure 1A and B). The windows were created using a 3D printer with gray resin, as previously reported for intravital imaging of female reproductive tracts [25]. The animal manipulation procedures in preparation for surgery were generally similar to previously described intravital surgical procedures in female mice [23]. The male mice were anesthetized with isoflurane by inhalation and maintained on the 37°C heating platform for the duration of the surgery and imaging. Ophthalmic ointment was applied to prevent eye dehydration during imaging. The fur on the lower abdomen over the testicular area was shaved, and a hair removal cream, Nair, was used to remove the hair. The depilated skin was swabbed with iodine solution and 70% ethanol three times. We removed a circular part of skin tissue with approximately 12 mm diameter and sutured the imaging window to the edge of the skin through 14 eyelets along the rim using 4–0 Nylon suture (Ethicon Inc). A ~5 mm incision was made in the muscle layer underneath the window to expose the reproductive organs. The testis and epididymis were gently pulled out and stabilized by securing the surrounding fat tissue onto the window tissue holders using a tiny droplet of surgical glue (Covetrus). A 37°C sterile saline solution was added to the exposed tissues to avoid dehydration before closure. The window was then closed with a 12 mm diameter circular cover glass and secured with an O-ring (Figure 1C). The entire surgical procedure was typically completed within 40 min.

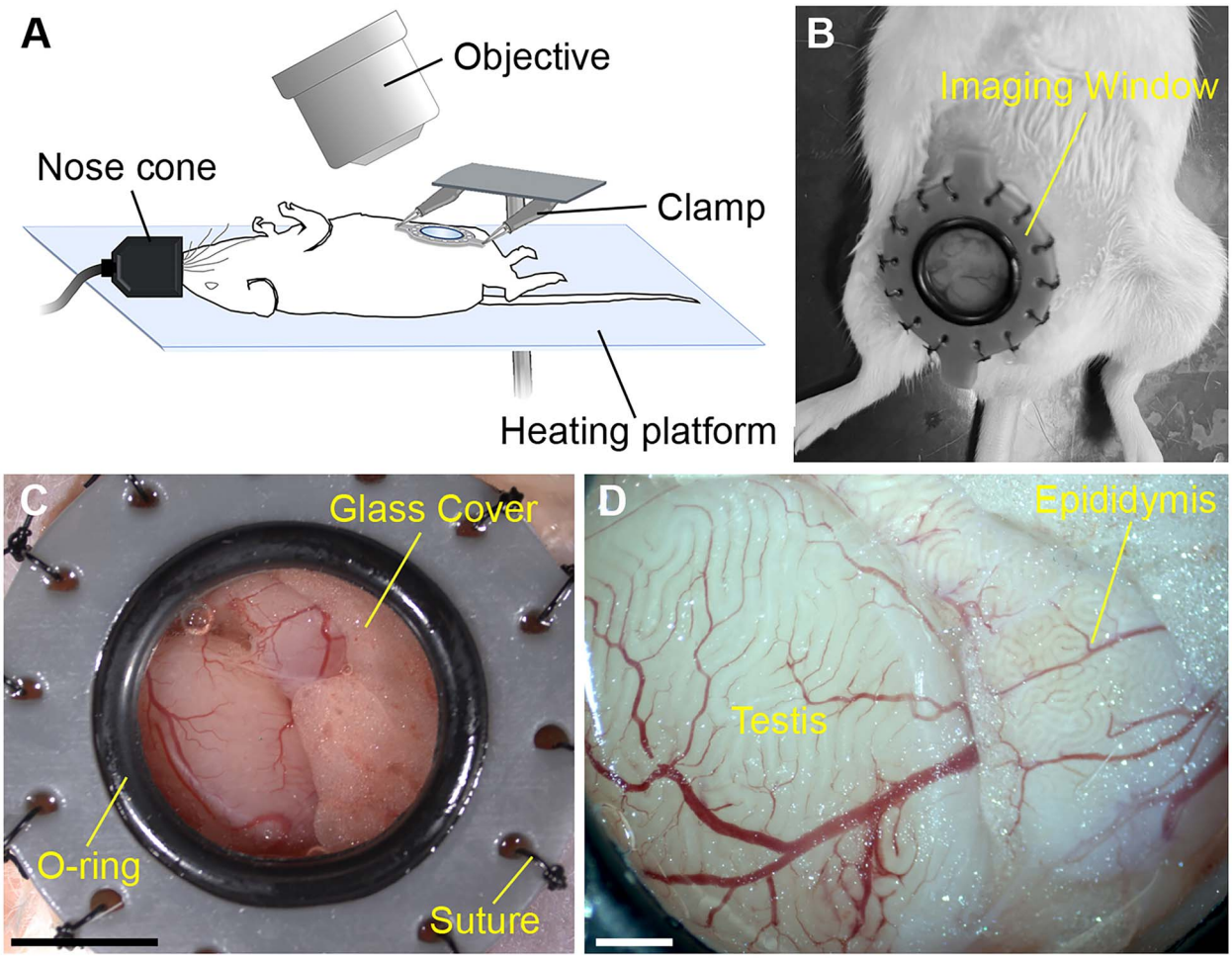

Figure 1. In vivo imaging of the mouse male reproductive organs with OCT through an implanted imaging window. (A) Schematic of the in vivo imaging setup. For in vivo OCT imaging, a male mouse was anesthetized with isoflurane via a nose cone and placed on the 37°C heating platform. The imaging window was stabilized with two clamps to minimize the influence of the body motion caused by breathing. (B) Image of a male mouse with the implanted imaging window. (C, D) Bright-field visualization of the testis and epididymis through the window in vivo. The scale bar in panel C corresponds to 5 mm, and the scale bars in panel D corresponds to 1 mm.

Upon completion of the surgery, the mouse was positioned on the OCT imaging stage. For the imaging, the window was stabilized with two clamps and slightly lifted to minimize movement artifacts due to animal breathing. In vivo OCT imaging of the testis and epididymis was conducted through the implanted abdominal window under anesthesia for up to 2 h (Figure 1D). The mice were sacrificed right after the imaging in the presented study.

Optical coherence tomography system and imaging

A house-built spectroscopic OCT system utilized in this study was previously described in [21]. Briefly, the system employs a supercontinuum laser (NKT Photonics) using a central wavelength of ~800 nm and a bandwidth of ~100 nm. A fiber-based Michaelson interferometer was employed, directing the interference of light from the reference and sample arms to a spectrometer based on a 250 kHz e2V OctoPlus camera (Teledyne Technologies Inc). Fast Fourier transform was used to obtain the OCT intensity A-line from the equally *k*-spaced interference fringes. The system provides an A-line rate of up to 250 kHz and has an axial and transverse resolutions of ~4 μm. The three-dimensional transverse scanning was performed using a set of galvanometer mirrors (GVS012, Thorlabs Inc), offering high flexibility in adjusting the number of pixels and the scanning distance. Various settings were applied to accommodate the size and structural differences in reproductive organ regions. Volumetric rendering and dynamic visualizations were conducted using Imaris software (Bitplane).

Analysis of tubular contractions in the testis and epididymis

Toward the investigation of tubular contractility, we performed dynamic in vivo OCT imaging of the testis and epididymis continuously for approximately 2–6 min. To determine the frequency of tubular contractions, a cross-sectional line through the tubule was selected from the volumetric dataset and plotted versus time. The contractions were clearly revealed as periodic changes in tubular position and diameter, allowing for the direct calculation of contraction frequency. We used five young mice and three aged mice for the analysis of contractions in the seminiferous tubules and epididymal duct, and at least three different regions were selected for the measurements on each mouse. The total number of measurements is included in the figure legends.

To quantify the contractile wave velocity along the tubule, we selected seven sequential cross-sectional positions along the caput epididymal duct from the acquired volume. At each cross-sectional position, a 2D time-lapse was exported, cropped to contain the tubule, and binarized to highlight the lumen; then, a noise reduction was performed using the *strel* function with a custom MATLAB code (The MathWorks Inc). The luminal cross-sectional area was calculated from the binary images and plotted over time for each position. The time of the peak in the luminal area was plotted against the distance of the corresponding cross-section along the tubule. A linear regression analysis between the peak times and the distances was performed to reveal the velocity of the tubular wave propagation.

Micro-computed tomography imaging

To set a reference for structural analysis of the reproductive system with OCT, we performed micro-computed tomography (micro-CT) imaging on the extracted male reproductive tract. After the dissection, the samples were fixed with 4% paraformaldehyde (Electron Microscopy Sciences) in phosphate-buffered saline (PBS) at 4°C for at least 24 h. The samples were transferred to a 1.5 ml tube containing 1 ml of X-CLARITY Hydrogel Solution (Logos Biosystems) with 0.25% X-CLARITY Polymerization Initiator (Logos Biosystems) and incubated at 4°C overnight for the polymer to diffuse through the samples. For the crosslinking, the samples were incubated at 37°C for 3 h. Then, we carefully cleared the specimens from external hydrogel and stored in PBS with 0.1% sodium azide (Sigma-Aldrich) at 4°C overnight. The samples were then immersed in 5 ml of 0.1 N iodine solution (Fisher Chemical) at 4°C until the micro-CT imaging for at least 2 days. We acquired the data on SKYSCAN 1272 (Bruker) as a set of 1921 images of 16.1 mm × 10.8 mm each with 4 μm/pixel. The X-ray source was set at 70 kV and 142 μA with a 0.5 mm aluminum filter. The acquired micro-CT data were reconstructed with NRecon software (Bruker) and then visualized with Imaris software (Bitplane). The seminiferous tubule diameter was measured using the Measurement Points function of Imaris software. The luminal area was measured using the Surfaces function of Imaris software.

Statistical analysis

Quantitative data on contraction frequency are presented as the mean ± standard error of the mean from measurements in at least three mice. Data analysis was conducted using GraphPad Prism 9 software. Unpaired Student *t*-test was used to analyze statistical differences in frequencies of seminiferous tubule contractions between young and aged mice. One-way ANOVA with Tukey's multiple comparison test was used to assess the significance of the differences in frequencies between epididymal regions. *P*-values less than 0.01 were considered statistically significant.

Results

In vivo volumetric imaging of mouse testis

We performed in vivo OCT imaging of the male reproductive organs through an implanted imaging window. For in vivo imaging, we surgically implanted a 3D-printed window on the male mouse to bypass skin and muscle layers and expose the male reproductive organs for imaging through an aperture covered with a glass coverslip (Figure 1A–D). The male reproductive organs were stabilized with a clamp throughout the imaging session to prevent movement artifacts caused by the animal's breathing (Figure 1A). Figure 2A shows a typical 3D OCT reconstruction of the mouse testis, illustrating its external morphology. Figure 2B presents a top-view cross-sectional image showing the coiled structure of seminiferous tubules tightly packed within the testis. The depth-resolved cross-sectional images of the seminiferous tubules are shown in Figure 2C and D. The lumen, germ cells, and the outer membrane of the testis were clearly visualized in vivo using OCT (Figure 2E). The quantitative measures acquired through the presented intravital OCT imaging were validated by comparative analysis of seminiferous tubule diameter with micro-CT images (Supplementary Figure S1). While micro-CT imaging does not allow for live visualization as intravital OCT, it is an established quantitative volumetric imaging technology that could be used for validation of OCT measurements in extracted tissues.

In vivo volumetric imaging of mouse epididymis

In vivo OCT imaging was performed on three different regions of the mouse epididymis. The 3D OCT reconstruction of caput, corpus, and cauda epididymis is shown in Figure 3A–C, respectively. Figure 3D–F presents top-view cross-sectional images showing the tightly packed epididymal duct within the epididymis in all three regions. The depth-resolved cross-sectional images of the epididymal duct in the caput, corpus, and cauda regions are shown in Figure 3G–I, respectively. The lumen of each duct and the connective tissue surrounding the epididymis were clearly identified in vivo (Figure 3J–L). These cross-sectional OCT images demonstrate a significant increase in the lumen diameter and area along the epididymal duct from the caput to the cauda (Supplementary Figure S2), which is consistent with a previous report using extracted organs [26]. Through comparative analysis of the luminal area in each epididymal region, we confirmed the correlation between the measurements acquired with intravital OCT images and micro-CT of extracted tissues (Supplementary Figure S2).

Sperm transport and seminiferous tubule contractions in vivo

Sperm transport begins in the seminiferous tubules within the testes, followed by transit through the efferent ducts and epididymis. To spatiotemporally capture the sperm transport through the seminiferous tubules in vivo, we performed 4D (3D + time) OCT imaging of mouse testes. Figure 4A shows time-lapse OCT images of the seminiferous tubules indicating the rapid transport of luminal contents through the tube (Supplementary Video S1). We also evaluated the temporal changes in image intensity of the acquired OCT cross-sections of the seminiferous tubules (Figure 4B–D). Figure 4C and D and Supplementary Video S2 show the frequency of tubal contractions that coincide with the luminal transport through the seminiferous tubules. The average frequency of seminiferous tubule contractions in young and aged mice was 6.3 ± 2.1 ($\times 10^{-3}$ Hz; $n = 27$) and 6.8 ± 2.5 ($\times 10^{-3}$ Hz; $n = 15$), respectively (Figure 4E). These results suggest that the presented OCT-based approach enables dynamic investigations of sperm transport and seminiferous tubule contractions in vivo, as well

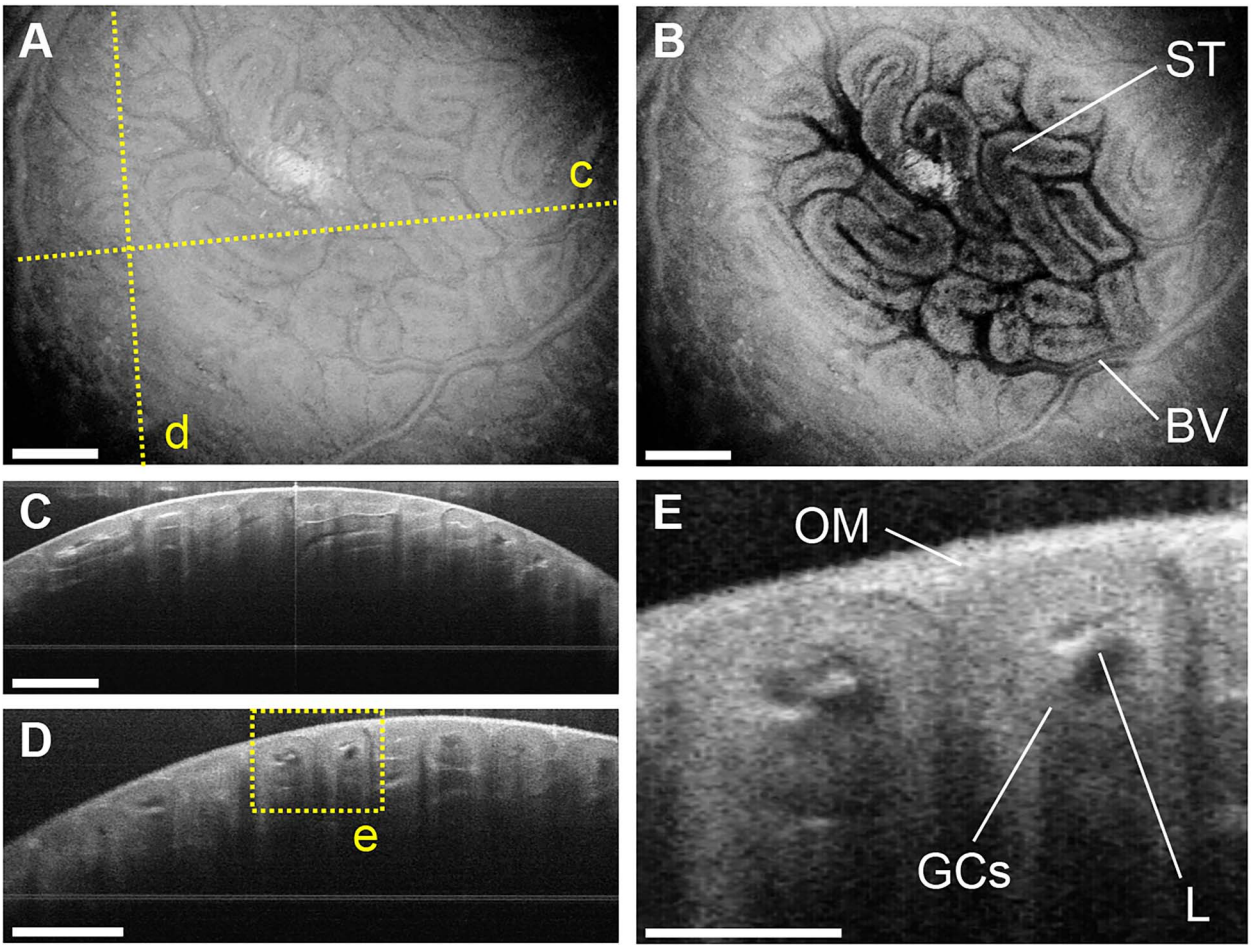

Figure 2. In vivo volumetric OCT imaging of the mouse testis. (A) Three-dimensional OCT rendering showing the external morphology of the testis. The dashed lines represent the locations for the cross-sections shown in panels C and D. (B) Top-view OCT cross-sectional images of the testis showing the seminiferous tubules (STs) and blood vessels (BVs). (C, D) Corresponding depth-resolved OCT cross-sections of the testis. The dashed rectangle represents the location for the higher-magnification images shown in panel E. (E) Depth-resolved OCT cross-sectional images of the seminiferous tubules inside the testis showing the germ cells (GCs), lumen (L), and outer membrane (OM). The scale bars in panels A–D correspond to 500 μm, and the scale bar in panel E corresponds to 200 μm.

as volumetric visualizations of microstructures of mouse testes dynamically.

Epididymal contractility in vivo

Smooth muscle contractions are responsible for sperm transport in the epididymis. We performed in vivo dynamic OCT imaging of the mouse epididymis to investigate its contractility. Figure 5A–F shows the temporal changes in tubular position and diameter of the acquired OCT cross-sectional lines from three different regions of the epididymis. The caput epididymis exhibits the highest frequency of contractions (Figure 5A and D), while the cauda epididymis shows the lowest frequency (Figure 5C and F), suggesting a decreasing contraction frequency from the caput to the cauda (Supplementary Videos S3–S5). To support this observation, we quantified the epididymal contractility and compared the contraction frequency among the three epididymal regions. The average frequency was 51.9 ± 4.7 ($\times 10^{-3}$ Hz; $n = 30$) in the caput, 27.1 ± 1.4 ($\times 10^{-3}$ Hz; $n = 30$) in the corpus, and 10.9 ± 1.4 ($\times 10^{-3}$ Hz; $n = 30$) in the cauda, indicating a significant variation in contraction frequency depending on the epididymal regions (Figure 5G), which is consistent with previous studies performed ex vivo [7–9]. In addition, we compared the frequency of the caput epididymal duct between young and aged mice to investigate the age-related changes in epididymal contractility in vivo. We did not observe significant difference in frequency between young and aged mice ($51.9 \pm 4.7 \times 10^{-3}$ Hz vs. $67.6 \pm 4.9 \times 10^{-3}$ Hz), suggesting that epididymal contractility remains functional until at least one to one and a half years of age.

Quantitative analysis of epididymal contraction wave associated with sperm transport

We conducted dynamic volumetric OCT imaging of the mouse caput epididymis to analyze the wave propagation of the contractions and sperm transport through the epididymal duct in vivo. Multiple positions were selected from the acquired volumetric dataset along the epididymal duct (Figure 6A). We obtained corresponding cross-sections at each position and quantified the luminal area over time to investigate the dynamics of the contractile wave. Figure 6B shows the temporal changes in the luminal area at each position, demonstrating a shift in the time points of the largest luminal area along the epididymal duct from P1 to P7, as indicated by arrows. This result suggests that the contraction wave propagated along the epididymal duct, corresponding to sperm transport through

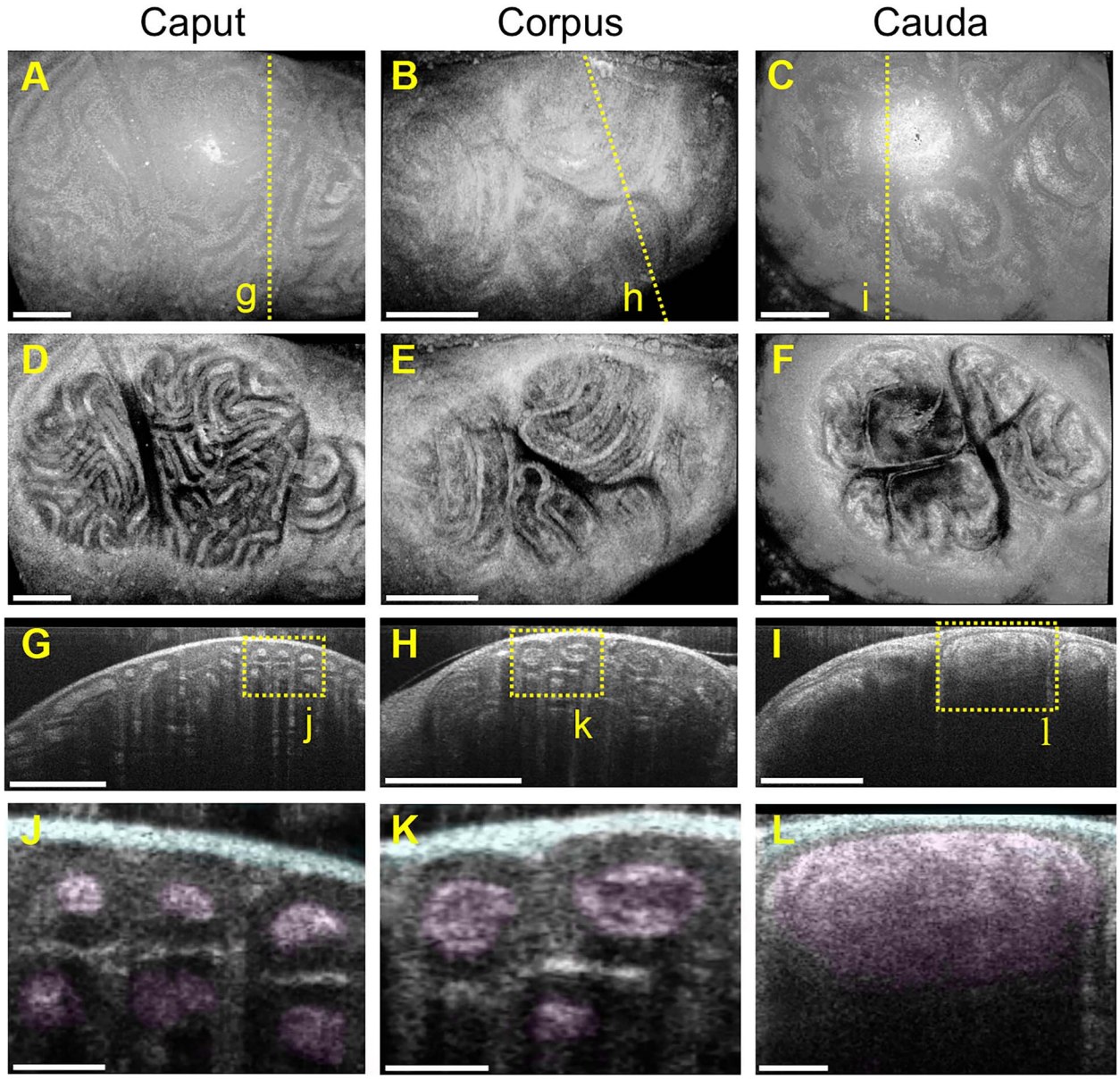

Figure 3. In vivo volumetric OCT imaging of the mouse epididymis. (A–C) Three-dimensional OCT reconstruction of the caput epididymis (A), corpus epididymis (B), and cauda epididymis (C). The dashed lines represent the locations for the cross-sections shown in panels G–I. (D–F) Top-view OCT cross-sectional images of the three different regions of the epididymis showing a tightly packed epididymal duct inside the organ. (G–I) Corresponding depth-resolved OCT cross-sections of the caput epididymis (G), corpus epididymis (H), and cauda epididymis (I). The dashed rectangles represent the locations for the higher-magnification images shown in panels J–L. (J–L) Depth-resolved OCT cross-sectional images of the caput epididymis (J), corpus epididymis (K), and cauda epididymis (L). The lumen and connective tissue surrounding the epididymis are highlighted. The scale bars in (A–I) correspond to 500 μm, and the scale bars in panels J–L correspond to 100 μm.

the duct (Supplementary Video S6). The average velocity of wave propagation was estimated as 204.1 ± 29.2 μm/s through linear regression analysis of the distance versus time delay at each position (Figure 6C). Taken together, these findings highlight the potential of this technology for studying epididymal dynamics, including sperm/luminal transport and smooth muscle contractions, in vivo in mouse models.

Discussion

In this study, we introduced a novel functional in vivo imaging approach using OCT, enabling label-free, depth-resolved, three-dimensional, high-resolution visualization of the mouse testis and epididymis. The structural features revealed by this approach were highly comparable to those obtained by ex vivo imaging using OCT, as previously reported [21]. The presented approach offers several advantages over previously used methods, including in vivo imaging capability, deeper imaging depth, a wide field of view, and no need for exogenous contrast agents. This allows one to investigate the male reproductive system with minimal alteration of its physiological environment. Since OCT light exposure is considered to be safe by the U.S. Food and Drug Administration and is widely used in ophthalmology and cardiology clinics [27], our approach may also minimize the influence of imaging light on the reproductive tissues. Taken together, the method presented

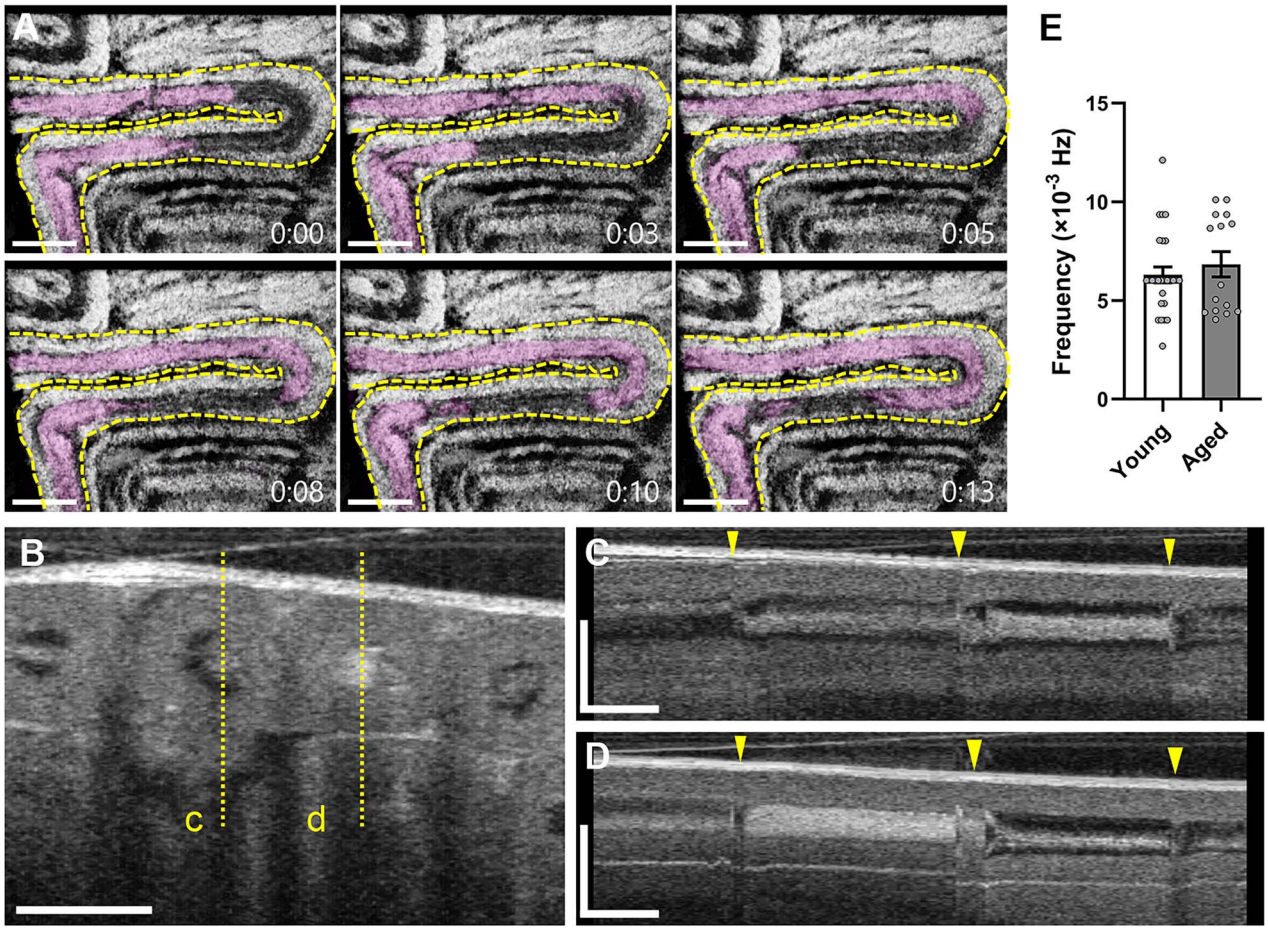

Figure 4. Sperm transport through the seminiferous tubules in vivo. (A) Time-lapse OCT images of the mouse testis showing the transfer of luminal contents through the seminiferous tubules. The dashed line represents the outline of the seminiferous tubule. The luminal contents are highlighted. The time stamps are coded as minutes:seconds. (B) Cross-sectional OCT image of the mouse testis. The dashed lines indicate the locations for the corresponding temporal mapping shown in panels C and D. (C, D) Temporal mapping of the corresponding seminiferous tubules showing the frequency of contractions that coincide with luminal transport. The arrow heads indicate the time points of seminiferous tubule contractions. (E) Comparison of the frequency in seminiferous tubule contractions between young and aged mice. Data are shown as the mean ± standard error with individual data points ($n = 27$ for young mice, $n = 15$ for aged mice). The scale bars in panels A and B correspond to 500 and 200 μm, respectively. The horizontal bars and vertical bars in panels C and D correspond to 60 s and 200 μm, respectively.

here provides a platform for a variety of future investigations on the reproductive process from a dynamic perspective. This method will be a useful tool for functional phenotyping in genetic mouse models with abnormalities in male reproductive structures, sperm transport, and tubular contractions, as well as for investigating the pharmacological and environmental effects on reproductive functions.

While OCT has multiple advantages for the dynamic investigation of physiological processes, it is associated with some limitations. The absence of a requirement for exogenous contrast is advantageous; however, it also poses a limitation because this feature does not provide an opportunity for molecular specificity, achievable by other technologies such as fluorescence microscopy. For that reason, for example, OCT imaging did not allow us to identify the different developmental stages of germ cells, which could be assessed in sections by confocal microscopy. Since resolution and imaging depth are linked, the higher imaging depth of OCT comes at the expense of lower spatial resolution than confocal and multiphoton microscopy, which poses another limitation. This limitation could be partially resolved by utilizing a higher-resolution optical coherence microscopy system [28]. Potentially, some of the limitations of OCT could also be solved by the implementation of multimodality designs. For example, photoacoustic tomography provides even higher imaging depth and allows for fast volumetric mapping of blood oxygenation; therefore, combining OCT with photoacoustic tomography [29] would allow one to study the ductal dynamics and sperm transfer in the context of the whole organ and to investigate the metabolic regulation of the reproductive system. Combining OCT imaging with elastography [30] or Brillouin microscopy [31] would provide mechanical contrast and allow one to explore the role of stiffness in reproductive organ development and spermatogenesis. Multimodal integration of OCT with light-sheet microscopy [32] or confocal/multiphoton microscopy would allow for molecular labeling and provide a powerful tool for spatiotemporal tracking of germ cell differentiation during spermatogenesis in the context of tubular dynamics and organ structure. Such multimodal approaches would synergistically combine the capabilities of each technology and bring comprehensive insights into reproductive physiology from both structural and functional aspects.

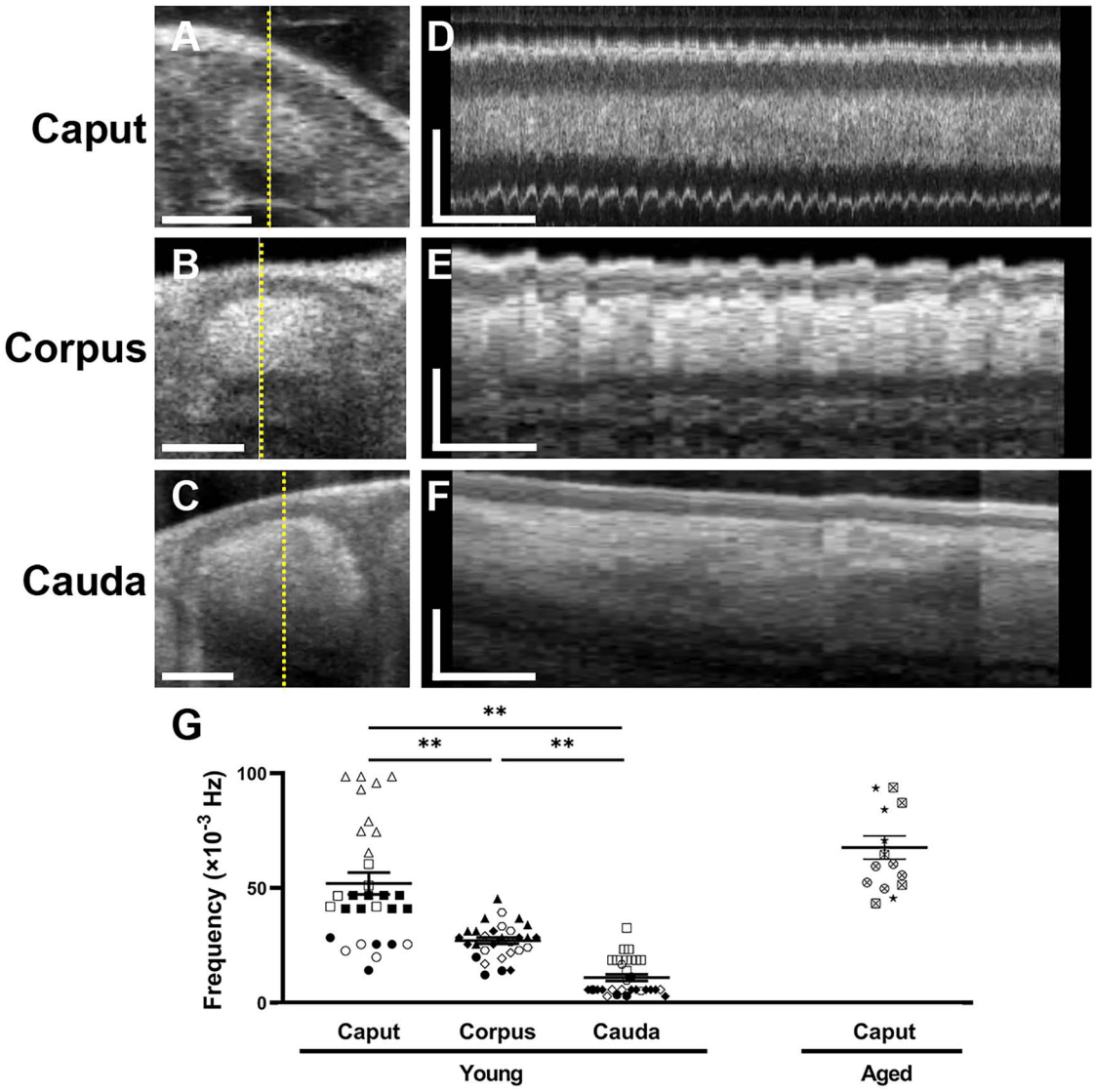

Figure 5. Epididymal contractility in vivo. (A–C) Depth-resolved OCT cross-sections of the caput epididymis (A), corpus epididymis (B), and cauda epididymis (C). The dashed lines indicate the locations for the corresponding temporal mapping shown in panels D–F. The scale bars in panels A–C correspond to 100 μm. (D–F) Temporal mapping of the corresponding cross-sectional lines showing the frequency of contractions in the three different regions of the epididymis. The horizontal bars and vertical bars in panels D–F correspond to 60 s and 100 μm, respectively. (G) Comparison of the contraction frequency in the three different epididymal regions. Data are shown as the mean ± standard error with individual data points ($n = 30$ for young mice, $n = 15$ for aged mice). The unique symbols (open, closed, and crossed circle, square, triangle, rhombus, hexagon, and star) represent individual animals. Statistical analysis by one-way ANOVA with Tukey's multiple comparisons test indicated significant differences between each group ($**P < 0.01$).

There are numerous potential applications for the presented approach. Sperm transport through the male reproductive tract is an essential reproductive process. Mammalian sperm undergo a series of post-testicular modifications and acquire motility during their transit through the epididymis [33]. Therefore, the disruption of appropriate regulation of sperm transport can lead to incomplete sperm maturation and male infertility. For example, both the acceleration and delay of sperm transit in the epididymis affect the sperm quality [34, 35]. Male rats treated with methylmercury showed significantly decreased transit time in the caput and corpus epididymis, which coincided with the reduction in progressively motile sperm obtained from the vas deferens [36]. Several imaging-based investigations have contributed to our understanding of this transport mechanism. Kanazawa et al. visualized the luminal flow in the seminiferous tubules, indicating that this physical force facilitates sperm release from Sertoli cells [13]. Fleck et al. visualized and quantified the spontaneous contractions of seminiferous tubules that push immotile sperm toward the rete testis and efferent duct [12]. Using video microscopy and a mouse model with disrupted ciliary activity, Aprea et al. demonstrated that ciliary beating plays an important role in sperm transport through the efferent duct in mice [5]. Multiple studies using time-lapse ex vivo imaging suggested that contractions of the epididymal duct are involved in luminal and sperm transport through the epididymis [7, 37, 38]. To measure the velocity of the intraluminal fluid, Turner et al. injected stained mineral oil into the rat epididymal duct using a micromanipulator and tracked the oil droplet using microscopy [39]. Intraluminal pressures or

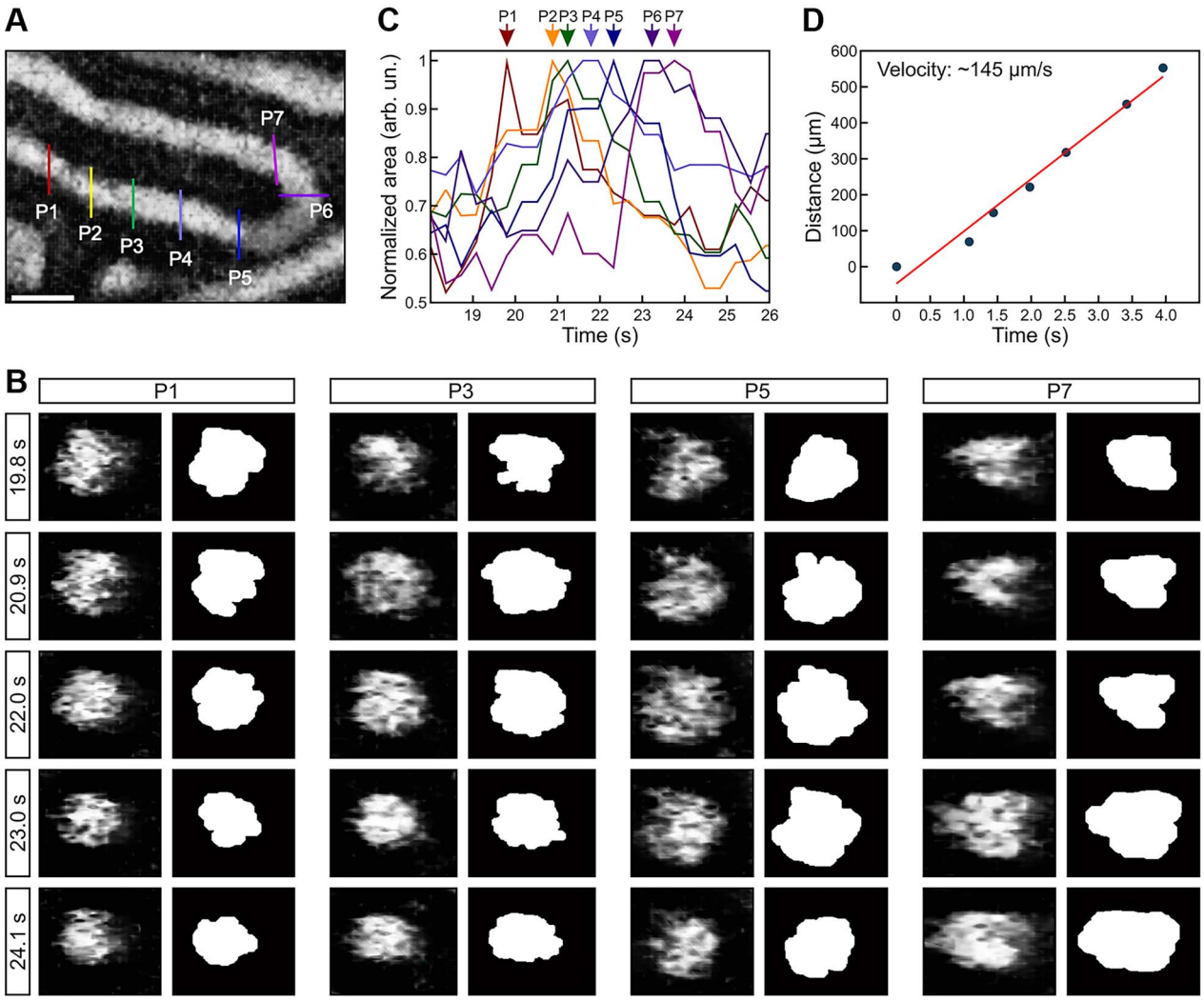

Figure 6. Luminal wave propagation through the caput epididymal duct. (A) Top-view OCT cross-sectional image of the epididymal duct. The color-coded lines indicate the positions (P1–P7) selected for the analysis of the luminal wave in the caput epididymis. (B) Representative OCT cross-sections and corresponding binary images over five time points. (C) Normalized luminal area profiles over time from the seven locations along the caput epididymis. The different positions P1-P7 were color-coded. (D) Quantification of the velocity of epididymal wave propagation. A linear regression on the data of the time delay vs. the distance of wave propagation provides an estimation of the wave velocity. The scale bar in panel A corresponds to 100 μm.

smooth muscle electrical activity were measured in different regions of the extracted rat epididymis to investigate the frequency and amplitude of contraction [9, 40]. Contractility of the epididymal duct was previously measured in extracted tubules with a force–displacement transducer, which allowed for the analysis of concentration–response curves to test the effect of drugs on epididymal contractility and to determine the potency and efficacy of different compounds [41, 42]. The presented intravital, volumetric, dynamic, structural, and functional OCT imaging complements the existing methods for the analysis of male reproductive physiology providing novel opportunities for studying sperm maturation and transport.

It is believed that the dynamics of the reproductive system, such as smooth muscle contractions, ciliary beating, and luminal fluid flow, are major contributors to sperm transport through the male reproductive tract. However, due to the lack of in vivo dynamic imaging technologies to capture these dynamics, there is still little information on the physiological and biomechanical regulations of sperm transport in the male reproductive tract. In this study, we spatiotemporally captured tubule contractions and luminal transport in the mouse testis and epididymis, as well as the microstructures of these reproductive organs, which is not currently achievable with other approaches. Our results suggest that epididymal contractility is dramatically distinct between epididymal regions (Figure 5). Specifically, the contraction frequency was significantly lower in the cauda epididymis in comparison to the caput epididymis, which is consistent with previous studies using extracted tissues studied in culture [7–9]. Based on gene expression, the epididymis can be further segmented into 10 different portions in adult mice and 19–20 segments in adult rats [43, 44]. However, OCT technology currently does not allow for molecular contrast and genetic reporter labeling. For this reason, without molecular specificity, epididymal regional segmentation beyond the caput, corpus, and cauda was not technologically possible in this study. Going forward, combining the presented intravital, volumetric, and dynamic OCT imaging with molecular labeling and genomic/transcriptomic analyses might provide novel insight into regional functional

differences and specific roles of epididymal segments in sperm maturation and transport, which is an important area for future investigation.

In addition to the contraction frequency, we also volumetrically visualized and quantified the luminal wave propagation along the caput epididymal duct (Figure 6). The average wave propagation velocity was estimated to be 204.1 μm/s. To our knowledge, there are no previous measurements of epididymal waves to compare to, but it is much slower than the velocity of the wave propagating along the oviduct [25]. Based on our observations, the waves repeatedly propagated in the same direction along the epididymal duct (Supplementary Videos S6 and S7). Although we do not know the direction of wave propagation due to the structural complexity of the epididymal duct, this observation is consistent with a previous study showing that the electrical activity in the middle part of the rat cauda epididymis periodically spreads in the same direction [9]. Time-lapse imaging also suggests the directional transport of luminal cells and exfoliated cells through the neonatal rat epididymis [38]. However, another previous study demonstrated bidirectional transportation of injected oil droplets through the rat epididymis in vitro [45], suggesting that epididymal contractions can spread in both directions. It is important to note that this manuscript presents a limited number of observations; therefore, we might have missed bidirectional waves if they present at specific regions and time points. Also, the corpus and cauda epididymal ducts are highly convoluted, making it difficult to follow the wave propagations in these regions of the epididymis, which might be distinct from others. These limitations could potentially be addressed by implementing the presented intravital approach in combination with either prolonged OCT imaging over a larger field of view or brightfield imaging and tracking of injected dye in the epididymal duct. Further investigations are necessary to fully understand the dynamics of the contraction wave and sperm transport throughout the epididymal duct and to examine how these region-dependent dynamics are related to sperm maturation and storage in vivo.

In conclusion, we present in vivo dynamic volumetric OCT imaging of the male mouse reproductive tract at a micro-level spatial resolution with millimeter-level imaging depth. To the best of our knowledge, this is the first functional imaging technology capable of in vivo dynamic investigations and three-dimensional visualizations of mammalian testes and epididymides. We performed in vivo quantitative measurements of tubular contractility and visualized sperm transport dynamically through the seminiferous tubules and epididymal duct, revealing the variety of physiological dynamics occurring within the male reproductive tract. Since much of our current knowledge is still largely derived from extrapolation of in vitro and ex vivo experiments and lacks direct in vivo evidence, these novel approaches would provide a platform for a variety of advanced studies in reproductive biology and medicine. Considering that many molecules affecting male fertility have been identified by genetic manipulation in mice [46, 47], dynamic imaging investigations under functionally disrupted conditions may be helpful in answering unexplored questions in mammalian reproduction. For example, interstitial cells of Cajal are known as pacemaker cells for smooth muscle contraction in the gut [48]. Although these cells are localized in the interstitial space of the mouse epididymis from the initial segment to the cauda, the physiological role of interstitial cells of Cajal in the epididymis remains unclear [49, 50]. The integration of the presented imaging approach with pharmacological activation or inhibition of specific signaling pathways may help to reveal the interplay between smooth muscle cells and interstitial cells and to explore the pacemaker cells in the epididymis. Such a combination of advanced imaging techniques and genetic, molecular, or pharmacological approaches would provide valuable insights and better strategies for the treatment of human infertility and other reproductive pathologies.

Supplementary material

Supplementary material is available at *BIOLRE* online.

Conflict of Interest

The authors have declared that no conflict of interest exists.

Author contributions

KU designed this study, conducted the experiments, acquired the data, and drafted the manuscript. GRM performed quantitative analysis and reviewed and revised the manuscript. IVL supervised this study and reviewed and revised the manuscript.

Data availability

The data underlying this article will be shared on reasonable request to the corresponding author.

References

1. Griswold MD. Spermatogenesis: the commitment to meiosis. *Physiol Rev* 2016; **96**:1–17.
2. James ER, Carrell DT, Aston KI, Jenkins TG, Yeste M, Salas-Huetos A. The role of the epididymis and the contribution of epididymosomes to mammalian reproduction. *Int J Mol Sci* 2020; **21**:5377.
3. Ellis LC, Groesbeck MD, Farr CH, Tesi RJ. Contractility of seminiferous tubules as related to sperm transport in the male. *Arch Androl* 1981; **6**:283–294.
4. Maekawa M, Kamimura K, Nagano T. Peritubular myoid cells in the testis: their structure and function. *Arch Histol Cytol* 1996; **59**: 1–13.
5. Aprea I, Nothe-Menchen T, Dougherty GW, Raidt J, Loges NT, Kaiser T, Wallmeier J, Olbrich H, Strunker T, Kliesch S, Pennekamp P, Omran H. Motility of efferent duct cilia aids passage of sperm cells through the male reproductive system. *Mol Hum Reprod* 2021; **27**:gaab009.
6. Hoque M, Kim EN, Chen D, Li FQ, Takemaru KI. Essential roles of efferent duct multicilia in male fertility. *Cell* 2022; **11**:11.
7. Elfgen V, Mietens A, Mewe M, Hau T, Middendorff R. Contractility of the epididymal duct—function, regulation and potential drug effects. *Reproduction* 2018; **156**:R125–R141.
8. Mewe M, Bauer CK, Schwarz JR, Middendorff R. Mechanisms regulating spontaneous contractions in the bovine epididymal duct. *Biol Reprod* 2006; **75**:651–659.
9. Talo A, Jaakkola UM, Markkula-Viitanen M. Spontaneous electrical activity of the rat epididymis in vitro. *J Reprod Fertil* 1979; **57**: 423–429.
10. Filippi S, Morelli A, Vignozzi L, Vannelli GB, Marini M, Ferruzzi P, Mancina R, Crescioli C, Mondaini N, Forti G, Ledda F, Maggi M. Oxytocin mediates the estrogen-dependent contractile activity of endothelin-1 in human and rabbit epididymis. *Endocrinology* 2005; **146**:3506–3517.

11. Mewe M, Wulfsen I, Middendorff R, Bauer CK. Differential modulation of bovine epididymal activity by oxytocin and noradrenaline. *Reproduction* 2007; **134**:493–501.
12. Fleck D, Kenzler L, Mundt N, Strauch M, Uesaka N, Moosmann R, Bruentgens F, Missel A, Mayerhofer A, Merhof D, Spehr J, Spehr M. ATP activation of peritubular cells drives testicular sperm transport. *Elife* 2021; **10**:10.
13. Kanazawa Y, Omotehara T, Nakata H, Hirashima T, Itoh M. Three-dimensional analysis and in vivo imaging for sperm release and transport in the murine seminiferous tubule. *Reproduction* 2022; **164**:9–18.
14. Roy J, Kim B, Hill E, Visconti P, Krapf D, Vinegoni C, Weissleder R, Brown D, Breton S. Tyrosine kinase-mediated axial motility of basal cells revealed by intravital imaging. *Nat Commun* 2016; **7**:10666.
15. Huang D, Swanson EA, Lin CP, Schuman JS, Stinson WG, Chang W, Hee MR, Flotte T, Gregory K, Puliafito CA, Fujimoto JG. Optical coherence tomography. *Science* 1991; **254**:1178–1181.
16. Scully DM, Larina IV. Mouse embryo phenotyping with optical coherence tomography. *Front Cell Dev Biol* 2022; **10**:1000237.
17. Umezu K, Larina IV. Optical coherence tomography for dynamic investigation of mammalian reproductive processes. *Mol Reprod Dev* 2023; **90**:3–13.
18. Wang S, Larina IV. Dynamics of gametes and embryos in the oviduct: what can in vivo imaging reveal? *Reproduction* 2023; **165**:R25–R37.
19. Trottmann M, Kolle S, Leeb R, Doering D, Reese S, Stief CG, Dulohery K, Leavy M, Kuznetsova J, Homann C, Sroka R. Ex vivo investigations on the potential of optical coherence tomography (OCT) as a diagnostic tool for reproductive medicine in a bovine model. *J Biophotonics* 2016; **9**:129–137.
20. Ramasamy R, Sterling J, Manzoor M, Salamoon B, Jain M, Fisher E, Li PS, Schlegel PN, Mukherjee S. Full field optical coherence tomography can identify spermatogenesis in a rodent sertoli-cell only model. *J Pathol Inform* 2012; **3**:4.
21. Umezu K, Xia T, Larina IV. Dynamic volumetric imaging and cilia beat mapping in the mouse male reproductive tract with optical coherence tomography. *Biomed Opt Express* 2022; **13**:3672–3684.
22. Wang S, Larina IV. In vivo three-dimensional tracking of sperm behaviors in the mouse oviduct. *Development* 2018; **145**:dev157685.
23. Wang S, Larina IV. In vivo dynamic 3D imaging of oocytes and embryos in the mouse oviduct. *Cell Rep* 2021; **36**:109382.
24. Wang S, Burton JC, Behringer RR, Larina IV. In vivo micro-scale tomography of ciliary behavior in the mammalian oviduct. *Sci Rep* 2015; **5**:13216.
25. Wang S, Syed R, Grishina OA, Larina IV. Prolonged in vivo functional assessment of the mouse oviduct using optical coherence tomography through a dorsal imaging window. *J Biophotonics* 2018; **11**:e201700316.
26. Nakata H, Iseki S. Three-dimensional structure of efferent and epididymal ducts in mice. *J Anat* 2019; **235**:271–280.
27. Zysk AM, Nguyen FT, Oldenburg AL, Marks DL, Boppart SA. Optical coherence tomography: a review of clinical development from bench to bedside. *J Biomed Opt* 2007; **12**:051403.
28. Karnowski K, Ajduk A, Wieloch B, Tamborski S, Krawiec K, Wojtkowski M, Szkulmowski M. Optical coherence microscopy as a novel, non-invasive method for the 4D live imaging of early mammalian embryos. *Sci Rep* 2017; **7**:4165.
29. Liu M, Maurer B, Hermann B, Zabihian B, Sandrian MG, Unterhuber A, Baumann B, Zhang EZ, Beard PC, Weninger WJ, Drexler W. Dual modality optical coherence and whole-body photoacoustic tomography imaging of chick embryos in multiple development stages. *Biomed Opt Express* 2014; **5**:3150–3159.
30. Wang S, Larin KV. Optical coherence elastography for tissue characterization: a review. *J Biophotonics* 2015; **8**:279–302.
31. Zhang J, Raghunathan R, Rippy J, Wu C, Finnell RH, Larin KV, Scarcelli G. Tissue biomechanics during cranial neural tube closure measured by Brillouin microscopy and optical coherence tomography. *Birth Defects Res* 2019; **111**:991–998.
32. Wu C, Le H, Ran S, Singh M, Larina IV, Mayerich D, Dickinson ME, Larin KV. Comparison and combination of rotational imaging optical coherence tomography and selective plane illumination microscopy for embryonic study. *Biomed Opt Express* 2017; **8**:4629–4639.
33. Dacheux JL, Dacheux F. New insights into epididymal function in relation to sperm maturation. *Reproduction* 2014; **147**:R27–R42.
34. Fernandez CD, Porto EM, Arena AC, Kempinas WG. Effects of altered epididymal sperm transit time on sperm quality. *Int J Androl* 2008; **31**:427–437.
35. Meistrich ML, Hughes TH, Bruce WR. Alteration of epididymal sperm transport and maturation in mice by oestrogen and testosterone. *Nature* 1975; **258**:145–147.
36. Fossato da Silva DA, Teixeira CT, Scarano WR, Favareto AP, Fernandez CD, Grotto D, Barbosa F Jr, Kempinas WG. Effects of methylmercury on male reproductive functions in Wistar rats. *Reprod Toxicol* 2011; **31**:431–439.
37. Mietens A, Tasch S, Stammler A, Konrad L, Feuerstacke C, Middendorff R. Time-lapse imaging as a tool to investigate contractility of the epididymal duct – effects of Cgmp signaling. *PloS One* 2014; **9**:e92603.
38. Weiser D, Mietens A, Stadler B, Ježek D, Schuler G, Middendorff R. Contractions transport exfoliated epithelial cells through the neonatal epididymis. *Reproduction* 2020; **160**:109–116.
39. Turner TT, Gleavy JL, Harris JM. Fluid movement in the lumen of the rat epididymis: effect of vasectomy and subsequent vasovasostomy. *J Androl* 1990; **11**:422–428.
40. Pholpramool C, Triphrom N, Din-Udom A. Intraluminal pressures in the seminiferous tubules and in different regions of the epididymis in the rat. *J Reprod Fertil* 1984; **71**:173–179.
41. Bezerra MS, Martins ABM, Trajano FMG, Pontes THA, Gomes L, Gavioli EC, Silva Junior EDD. Fluoxetine and sertraline effects on rat distal cauda epididymis contraction, sperm count and sperm transit time trough epididymis. *Eur J Pharmacol* 2019; **865**:172774.
42. da Silva Junior ED, de Souza BP, Vilela VV, Rodrigues JQ, Nichi M, de Agostini Losano JD, Dalmazzo A, Barnabe VH, Jurkiewicz A, Jurkiewicz NH. Epididymal contraction and sperm parameters are affected by clonidine. *Andrology* 2014; **2**:955–966.
43. Domeniconi RF, Souza AC, Xu B, Washington AM, Hinton BT. Is the epididymis a series of organs placed side by side? *Biol Reprod* 2016; **95**:10.
44. Johnston DS, Jelinsky SA, Bang HJ, DiCandeloro P, Wilson E, Kopf GS, Turner TT. The mouse epididymal transcriptome: transcriptional profiling of segmental gene expression in the epididymis. *Biol Reprod* 2005; **73**:404–413.
45. Jaakkola UM, Talo A. Movements of the luminal contents in two different regions of the caput epididymidis of the rat in vitro. *J Physiol* 1983; **336**:453–463.
46. Okabe M. The cell biology of mammalian fertilization. *Development* 2013; **140**:4471–4479.
47. Okabe M. Sperm-egg interaction and fertilization: past, present, and future. *Biol Reprod* 2018; **99**:134–146.
48. Takaki M. Gut pacemaker cells: the interstitial cells of Cajal (ICC). *J Smooth Muscle Res* 2003; **39**:137–161.
49. Hiroshige T, Uemura KI, Hirashima S, Hino K, Togo A, Ohta K, Igawa T, Nakamura KI. Morphological analysis of interstitial cells in murine epididymis using light microscopy and transmission electron microscopy. *Acta Histochem* 2021; **123**:151761.
50. Lee V, Hinton BT, Hirashima T. Collective cell dynamics and luminal fluid flow in the epididymis: a mechanobiological perspective. *Andrology* 2023; 1–10.